Brief paper

Cooperative moving path following for multiple fixed-wing unmanned aerial vehicles with speed constraints☆

Yuanzhe Wang, Danwei Wang *, Senqiang Zhu

School of Electrical and Electronic Engineering, Nanyang Technological University, 639798 Singapore, Singapore

A R T I C L E   I N F O

A B S T R A C T

This paper is to address a cooperative moving path following (CMPF) problem, in which a fleet of fixed-wing unmanned aerial vehicles (UAVs) are required to converge to and follow a desired geometric moving path while satisfying prespecified speed and spatial constraints. A representative application of the CMPF problem is the challenging mission scenario where a group of UAVs are tasked to track a moving ground target. The proposed methodology is based on the insight that a vehicle can follow a given path only through attitude control, thus leaving its speed as an extra input to be used at the coordination level. To deal with moving path following (MPF) of a single UAV, a non-singular control law is derived to steer the vehicle along the desired moving path which avoids the singularity problem in the previous MPF strategy. For multi-UAV coordination, a pursuit strategy is employed with the introduction of a virtual leader. To account for speed constraints and collision avoidance, conditions are derived under which the combined MPF and multi-UAV coordination closed-loop system is asymptotically stable while speed and spatial constraints are satisfied. Further simulation has been performed to demonstrate the effectiveness of the proposed method.

1. Introduction

A typical task for unmanned aerial vehicles (UAVs) is to converge to and follow a desired geometric path in order to accomplish military and rescue missions such as border patrolling, area surveillance and convoy protection. Due to its practical significance, path following of unmanned vehicles has been investigated extensively for many years. A seminal study of path following for unicycle-type vehicles is Micaelli and Samson (1993) where the path following error dynamics was defined using the Serret–Frenet frame concept. However, stringent initial condition constraints should be satisfied in the proposed strategy. To overcome this problem, a new type of non-singular path following control law was derived in Lapierre, Soetanto, and Pascoal (2006) and Soetanto, Lapierre, and Pascoal (2003) where global convergence of the path following error can be achieved. An alternative solution for the path following problem is the vector field approach and Refs. Griffiths (2006) and Nelson, Barber, McLain, and Beard (2007) are some pioneering work along this direction. To account for input

constraints of UAVs, control laws were derived in Beard, Ferrin, and Humpherys (2014) using the theory of nested saturations to follow straight lines and circular orbits. A recent survey for existing path following algorithms in two dimensional space of UAVs was presented in Sujit, Saripalli, and Sousa (2014), where five representative algorithms were introduced and analyzed. In classical path following problems, the reference path is stationary with respect to the inertial coordinate frame. However, in some practical applications such as moving target monitoring, convoy protection, source seeking, etc., UAVs are generally required to follow a path attached on a moving reference frame. And it has been analyzed in Oliveira, Aguiar, and Encarnação (2016) that classical path following algorithms cannot be directly applied to such problems. To fill this gap, moving path following (MPF) problem was first introduced in Oliveira et al. (2016) while a Lyapunov-based control law was derived for the UAV. Nevertheless, Oliveira et al. (2016) pointed out that the proposed control law is under the assumption that the vehicle will not be exactly at the distance from the closest path point that corresponds to the inverse of the path's curvature at that point. Intuitively, this assumption is hard to be satisfied just as a vehicle is very likely to occur at the center of a circular arc.

In practical applications, researchers and engineers prefer to using multiple small and low-cost UAVs to accomplish complicated missions due to the high efficiency for task completion and the robustness in the presence of vehicle failures. When multiple

---

vehicles are employed in a MPF scenario, a new motion control problem, cooperative moving path following (CMPF) problem, can be defined, in which a fleet of vehicles are required to converge to and follow a desired geometric moving path while satisfying prespecified speed and spatial constraints. Unlike path following problem, classical cooperative path following problem has received relatively less attention in the literature. Some representative results are Cichella et al. (2016, 2015), Lapierre, Soetanto, and Pascoal (2003), Xargay et al. (2012, 2013). A pioneer attempt for cooperative path following problem is Lapierre et al. (2003), where two underwater vehicles were required to move along two identical parallel paths with constant lateral distance using a leader–follower architecture. In Xargay et al. (2012), a new concept called virtual time was defined as the coordination state for each vehicle, based on which decentralized time-critical cooperative path following was achieved. Ref. Cichella et al. (2015) further investigated the cooperative path following problem when faulty communication networks, temporary link losses and switching topologies were considered. A comprehensive survey of cooperative path following algorithms was presented in Cichella et al. (2016). Among these existing results, vehicles are required to follow a set of desired spatial paths which are generated using cooperative path generation algorithms in advance as was illustrated in Cichella et al. (2016, 2015) and Xargay et al. (2012). However, considering potential applications of the CMPF problem such as target tracking, convoy protection and source seeking, the desired path is generally a closed curve which implies that all vehicles should move on the same path. Therefore, classical cooperative path following approaches cannot be directly extended to CMPF problem. Currently, there are already some results, such as Frew, Lawrence, and Morris (2008), Summers, Akella, and Mears (2009) and Yu and Liu (2017), dealing with cooperative moving target tracking problems which are similar to the CMPF problem studied in this paper. However, in these work, vehicles try to follow a circular path attached on the moving target and the approaches employed are not applicable to general curved paths.

In this paper, the CMPF problem for multiple fixed-wing UAVs is investigated while speed constraints imposed by physical limitations of the vehicles and collision avoidance are explicitly taken into consideration. The proposed methodology extends the previous work of MPF problem to CMPF scenarios. For single UAV MPF, a non-singular control law is proposed to steer the vehicle to converge to and move along the desired path, thus avoiding the singularity problem that arises when the position of the virtual target is simply defined by the projection of the vehicle on the path as in Oliveira et al. (2016). For the coordination part, a pursuit strategy is employed with the introduction of a virtual leader which moves with a constant speed along the given path. Vehicle speed is adjusted to maintain a constant along-path separation distance between neighboring vehicles. To account for speed and spatial constraints, conditions are provided in order to guarantee that the combined MPF and multi-UAV coordination closed-loop system is asymptotically stable while constraints are satisfied. Simulation results have also been provided to demonstrate the efficacy of the proposed strategy.

The main contributions of this paper are as follows:

(1) The CMPF problem is first introduced and formulated;
(2) A non-singular MPF control law is proposed which avoids the singularity problem in Oliveira et al. (2016), while robustness against wind measurement error is briefly analyzed;
(3) A coordination strategy is designed for UAVs to maintain a constant along-path separation distance between neighboring vehicles;

(4) Stability analysis of the combined MPF and multi-UAV coordination closed-loop system with speed and spatial constraints is provided.

The remainder of this paper is organized as follows. Section 2 formulates the CMPF problem. Section 3 presents the main results of this paper. Simulation results are given in Section 4. Final conclusions and future work are provided in Section 5.

2. Problem formulation

This section presents a mathematically rigorous formulation of the CMPF problem. First, for a single UAV, the MPF error dynamics is derived. Then, the objectives of the multi-UAV coordination mission are characterized.

To formulate the problem, three coordinate frames, inertial frame, path transport frame and Serret–Frenet frame, are considered. Inertial frame is represented as $\{I\} = \{\vec{x}, \vec{y}\}$ with $\vec{x}$ pointing east and $\vec{y}$ north. The origin of the path transport frame $\{P\} = \{\vec{x}_P, \vec{y}_P\}$ is $\boldsymbol{p}_P = [x_P, y_P]^T$ expressed in $\{I\}$. $\{P\}$ also moves in $\{I\}$ with velocity $\boldsymbol{v}_P = \dot{\boldsymbol{p}}_P = [v_{Px}, v_{Py}]^T$ and angular velocity ω_P both expressed in $\{I\}$. ψ_P is the heading angle of $\vec{x}_P$ in $\{I\}$. $^P\boldsymbol{p}_F(l) = [^Px_F(l), {}^Py_F(l)]^T$ is a desired planar geometric path parameterized by l, which is chosen as the arc length. $\{F\} = \{\vec{t}, \vec{n}\}$ is the Serret–Frenet frame associated to the desired path, $\kappa(l)$ is the path curvature and ψ_F is the heading angle of $\vec{t}$ in $\{I\}$. Actually, $\{F\}$ plays the role of a virtual target that should be tracked both in position and heading angle by the vehicle. Fig. 1 illustrates the relative position relationships among $\{I\}$, $\{P\}$ and $\{F\}$.

In this paper, the pre-superscript is employed to describe the coordinate frame in which the corresponding variable is expressed. For example, $^F\boldsymbol{p}$ represents the vehicle position with respect to $\{F\}$. For a variable without pre-superscript, it means that this variable is defined with respect to $\{I\}$. To deal with multiple UAVs, a subscript i is added to indicate the identity of the vehicle. For example, the heading angle of vehicle i is represented by ψ_i.

2.1. MPF error dynamics for a single UAV

In this subsection, the MPF error dynamics is presented. As this subsection only considers one UAV, the subscript i is omitted. The kinematic model of the fixed-wing UAV considered in this paper is given by

$$
\begin{aligned}
\dot{x} &= v \cos \psi + v_w \cos \psi_w \\
\dot{y} &= v \sin \psi + v_w \sin \psi_w , \\
\dot{\psi} &= \omega
\end{aligned}
\tag{1}
$$

where $\boldsymbol{p} = [x, y]^T$ is the vehicle position, v and ω are the airspeed and heading rate of the vehicle respectively, ψ is the heading angle of the vehicle, v_w is the wind speed, and ψ_w is the heading angle of the wind direction. Generally, vehicle speed and heading rate should satisfy $0 < v_{\min} \leq v \leq v_{\max}$, $-\omega_{\max} \leq \omega \leq \omega_{\max}$. In addition, vehicle position with respect to $\{F\}$ is denoted by $^F\boldsymbol{p} = [^Fx, {}^Fy]^T$, which indicates the MPF position error of the vehicle.

To facilitate the controller design, the dynamics of $^F\boldsymbol{p}$ will be derived in the sequel. First, consider a fixed point on $^P\boldsymbol{p}_F(l)$, which can be expressed in $\{I\}$ as $\boldsymbol{p}_F = \boldsymbol{p}_P + {}^IR_P{}^P\boldsymbol{p}_F$, where $^IR_P = \begin{bmatrix} \cos \psi_P & -\sin \psi_P \\ \sin \psi_P & \cos \psi_P \end{bmatrix}$ is the rotation transformation from $\{P\}$ to $\{I\}$. Then, by taking the time derivative and combining with the fact that $\boldsymbol{v}_P = \dot{\boldsymbol{p}}_P$ and $^P\dot{\boldsymbol{p}}_F = \boldsymbol{0}$, it can be obtained that $\dot{\boldsymbol{p}}_F = \boldsymbol{v}_P + S(\omega_P)(\boldsymbol{p}_F - \boldsymbol{p}_P)$, where $S(\omega_P) = \begin{bmatrix} 0 & -\omega_P \\ \omega_P & 0 \end{bmatrix}$, which describes the velocity of a fixed point on the path expressed in $\{I\}$ caused by the movement of $\{P\}$. Consequently, for a moving point on $^P\boldsymbol{p}_F(l)$ with
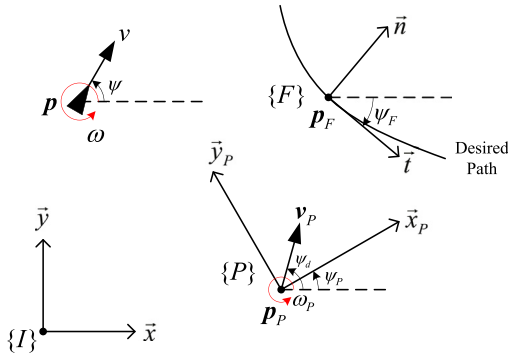
Fig. 1. Relative position relationships among {I}, {P} and {F}.

velocity ${}^F\mathbf{v}_F = [\dot{l}, 0]^T$ expressed in {F}, the velocity of that point with respect to {I} and expressed in {F} can be presented as

$${}^F R_I \dot{\mathbf{p}}_F = {}^F\mathbf{v}_F + {}^F R_I[\mathbf{v}_P + S(\omega_P)(\mathbf{p}_F - \mathbf{p}_P)]. \tag{2}$$

In addition, considering the rotation of {P}, the angular velocity of {F} with respect to {I} and expressed in {F} can be given by

$${}^F\omega_F = \omega_P + \kappa_l \dot{l}. \tag{3}$$

For a vehicle with position $\mathbf{p}$ expressed in {I} and position ${}^F\mathbf{p}$ with respect to {F}, it is obvious that $\mathbf{p} = \mathbf{p}_F + {}^I R_F {}^F\mathbf{p}$, from which it can be easily derived that

$${}^F\dot{\mathbf{p}} = {}^F R_I \dot{\mathbf{p}} - {}^F R_I \dot{\mathbf{p}}_F - S({}^F\omega_F){}^F\mathbf{p}. \tag{4}$$

For elegance of expression, the following notations are adopted.

$$\mathbf{p}_F - \mathbf{p}_P = [\Delta x, \Delta y]^T, \quad \bar{\psi} = \psi - \psi_F, \quad \bar{\psi}_w = \psi_w - \psi_F. \tag{5}$$

Based on the discussions above, the MPF error dynamics can be derived as follows.

$$\begin{aligned}
{}^F\dot{x} &= v\cos\bar{\psi} + {}^F\omega_F {}^Fy - \dot{l} + \Sigma \\
{}^F\dot{y} &= v\sin\bar{\psi} - {}^F\omega_F {}^Fx + \Delta \\
\dot{\tilde{\psi}} &= \omega - \omega_P - \kappa_l \dot{l} - \dot{\bar{\psi}}_d
\end{aligned} \tag{6}$$

where $\Sigma = v_w \cos\bar{\psi}_w - (v_{Px} - \omega_P \Delta y)\cos\psi_F - (v_{Py} + \omega_P \Delta x)\sin\psi_F$, $\Delta = v_w \sin\bar{\psi}_w + (v_{Px} - \omega_P \Delta y)\sin\psi_F - (v_{Py} + \omega_P \Delta x)\cos\psi_F$, $\tilde{\psi} = \bar{\psi} - \bar{\psi}_d$ is the attitude error and $\bar{\psi}_d$ is the desired heading error. Physically, Σ and Δ are the tangential and normal components of the disturbance term including v_w and the velocity of the virtual target caused by the movement of {P}, respectively. For notational convenience, define $\mathbf{e} = [{}^Fx, {}^Fy, \tilde{\psi}]^T$ to represent the MPF error. Before proceeding further, $\bar{\psi}_d$ will be detailed in the following.

First, the desired heading error ζ for $\bar{\psi}$ caused by Δ is defined as

$$\zeta = -\arcsin\frac{\Delta}{v}. \tag{7}$$

Physically, v should be larger than $|\Delta|$ such that the vehicle has enough capability to catch up with the desired moving path. Mathematically, $|\Delta| \leq v$ should be guaranteed. To this end, the following assumption is given.

$$|\Delta| \leq v\sin\theta_\zeta, \quad \theta_\zeta < \frac{\pi}{2}. \tag{8}$$

From (7) and (8), it can be obtained that $|\zeta| \leq \theta_\zeta$. To explicitly describe the constraints on the desired path, the upper bound of $|\Delta|$ should be derived. Assume that the movement of {P} satisfies $v_{Px} = v_d \cos\psi_d$, $v_{Py} = v_d \sin\psi_d$. Thus, $\Delta = v_d \sin(\psi_F - \psi_d) + v_w \sin\bar{\psi}_w - \omega_P\sqrt{\Delta x^2 + \Delta y^2}\sin(\psi_F + \varphi)$, where $\varphi = \arctan\frac{\Delta x}{\Delta y}$, from which

it can be obtained that $|\Delta| \leq \bar{\Delta} = v_d + \omega_P(\sqrt{\Delta x^2 + \Delta y^2})_{max} + v_w$. Consequently, to satisfy (8), a sufficient condition is given as follows.

$$\bar{\Delta} \leq v_{min}\sin\theta_\zeta. \tag{9}$$

Next, to achieve smooth convergence of the vehicle to the desired path, the transient maneuver is shaped as a function of ${}^Fy$. Hence, the desired heading error introduced by the expected transient maneuver is given as

$$\delta = -\theta_\delta \tanh(k_\delta {}^Fy), \tag{10}$$

where k_δ is a positive constant, $\theta_\delta = \bar{\theta} - \theta_\zeta$ and $\theta_\zeta < \bar{\theta} < \frac{\pi}{2}$. Above all, the desired heading error can be defined as

$$\bar{\psi}_d = \zeta + \delta. \tag{11}$$

From the discussions above, it can be found that $|\bar{\psi}_d| \leq |\zeta| + |\delta| \leq \theta_\zeta + \theta_\delta = \bar{\theta} < \frac{\pi}{2}$.

Now the MPF problem can be defined as follows.

Definition 1 (*MPF Problem*). Considering a UAV modeled by (1) moving with arbitrary feasible speed and a desired moving path ${}^P\mathbf{p}_F(l)$, design a MPF control law for ω, such that (1) ${}^Fx$, ${}^Fy$ and $\bar{\psi}$ are bounded; (2) $\mathbf{e}$ converge to zero asymptotically.

2.2. Coordination variable and information architecture

For potential applications of the CMPF problem like target monitoring, convoy protection and source seeking, vehicles are generally required to move along the desired path in a queue with a constant speed and a constant along-path separation distance. Considering the objectives of the coordination mission of n vehicles, a pursuit strategy is employed in this paper, where vehicle i pursues vehicle $i - 1$. For supplement, a virtual leader which is numbered as 0 and travels with a constant speed v_0 is introduced.

As one of the coordination objective is to maintain a constant along-path separation distance among vehicles, the arc length parameter is utilized to define the coordination variable. Suppose that l_i is the curvilinear abscissa of the ith virtual target tracked by vehicle i, which is an approximate metric for vehicle coordination, and therefore can be defined as the coordination variable. To meet the desired coordination requirement, it should be achieved that $\tilde{l}_i = 0$, $i = 1, 2, \ldots, n$, where $\tilde{l}_i = l_i - l_{i-1} + \Delta_l$ is the coordination error of vehicle i and Δ_l is the desired along-path separation distance.

For the information architecture of the multi-vehicle system, considering the pursuit strategy employed, vehicle i only receives information from vehicle $i - 1$ and only sends information to vehicle $i + 1$. This simple communication structure will be helpful for the reduction of communication burden among vehicles and the real-time operation of the whole system.

Based on the previous formulations, the CMPF problem for a fleet of UAVs can thus be defined as follows.

Definition 2 (*CMPF Problem*). Given a fleet of n UAVs modeled by (1) and a desired moving path ${}^P\mathbf{p}_F(l)$, design control laws of heading rate ω_i and speed v_i for each vehicle i, $i = 1, 2, \ldots, n$, such that (1) ${}^Fx_i$, ${}^Fy_i$, $\tilde{\psi}_i$ and $\tilde{l}_i$ are bounded; (2) $\mathbf{e}_i$ and $\tilde{l}_i$ converge to zero asymptotically; (3) constraints $0 < v_{min} \leq v \leq v_{max}$ and $\|\mathbf{p}_{i-1} - \mathbf{p}_i\| \geq S$, where S is the safe distance which should be larger than the diameter of the UAV, are satisfied.

3. Main results

This section presents the main results of this paper. First, the MPF problem for a single UAV is discussed. Then, the coordination among multiple UAVs is addressed. Finally, the stability of the combined MPF and multi-UAV coordination closed-loop system is analyzed while speed constraints and collision-free maneuvers for the vehicles are discussed.

3.1. MPF for a single UAV

A pioneering study of MPF for a UAV can be found in Oliveira et al. (2016), where a generic path following controller is proposed for a UAV at the kinematic level. In the proposed control law, the position of the virtual target, is placed at the closest point on the desired moving path from the real vehicle. Consequently, the proposed controller suffers from a singularity problem as pointed out in Oliveira et al. (2016), where a rather conservative assumption is made to avoid this singularity, which severely limits the practical application of the proposed controller. In this subsection, a non-singular path following control law is proposed through explicitly controlling the progression rate of the virtual target, thus bypassing the singularity problem.

To solve the MPF problem, let the rate of progression of the virtual target along the desired path be governed by

$$\dot{l} = v\cos\bar{\psi} + \Sigma + k_1{}^F x, \tag{12}$$

where k_1 is a positive constant. Then, the MPF control law is given as

$$\dot{\psi} = \omega_P + \kappa_l\dot{l} + \dot{\bar{\psi}}_d - \gamma{}^F y v \frac{\sin\bar{\psi} - \sin\bar{\psi}_d}{\bar{\psi} - \bar{\psi}_d} - k_2\tilde{\psi}, \tag{13}$$

where γ and k_2 are also positive constants. It should be noted that the term $\frac{\sin\bar{\psi} - \sin\bar{\psi}_d}{\bar{\psi} - \bar{\psi}_d}$ in (13) will not cause singularity. The detailed properties of this term are provided in our paper (Wang & Wang, 2017). Thus, the MPF closed-loop system can be presented as

$$\dot{e} = f(e), \tag{14}$$

where $f(e) = [-k_1{}^F x + {}^F\omega_F{}^F y, v\sin\bar{\psi} - {}^F\omega_F{}^F x + \Delta, -\gamma{}^F y v\frac{\sin\bar{\psi} - \sin\bar{\psi}_d}{\bar{\psi} - \bar{\psi}_d} - k_2\tilde{\psi}]^T$.

According to (13), the steady-state value of the control law (when $e = 0$) can be given as $\dot{\psi} = \omega_P + \kappa_l\dot{l} + \dot{\bar{\psi}}_d$. By taking into account the heading rate constraints at steady state, the following condition should be satisfied

$$|\omega_P + \kappa_l\dot{l} + \dot{\bar{\psi}}_d| \le \omega_{max}. \tag{15}$$

From (13), it can be found that $\dot{\bar{\psi}}_d$ is necessary in the control law computation. Based on the definition of $\bar{\psi}_d$, $\dot{\bar{\psi}}_d$ can be derived as

$$\dot{\bar{\psi}}_d = -\theta_\delta k_\delta \mathrm{sech}^2(k_\delta{}^F y){}^F\dot{y} - \frac{\dot{\Delta}}{\sqrt{v^2 - \Delta^2}} + \frac{\Delta\dot{v}}{v\sqrt{v^2 - \Delta^2}}, \tag{16}$$

where $\dot{\Delta} = \dot{v}_d\sin(\psi_F - \psi_d) + v_d({}^F\omega_F - \dot{\psi}_d)\cos(\psi_F - \psi_d) + (\omega_P{}^F\omega_F\Delta x - \dot{\omega}_P\Delta y - \omega_P\Delta\dot{y})\sin\psi_F + (-\omega_P{}^F\omega_F\Delta y - \dot{\omega}_P\Delta x - \omega_P\Delta\dot{x})\cos\psi_F + \dot{v}_w\sin\psi_w + v_w(\dot{\psi}_w - {}^F\omega_F)\cos\psi_w$. It should be noted that in (16), v_d, $\dot{v}_d$, ψ_d, $\dot{\psi}_d$, ω_P, $\dot{\omega}_P$, v_w, $\dot{v}_w$, ψ_w and $\dot{\psi}_w$ are the movement information of $\{P\}$ and wind, which are available for the control law computation. Besides, according to (2), $\Delta\dot{x}$ and $\Delta\dot{y}$ can be derived as $\Delta\dot{x} = \dot{l}\cos\psi_F - \omega_P\Delta y$ and $\Delta\dot{y} = \dot{l}\sin\psi_F + \omega_P\Delta x$.

Remark 1. For MPF problem of a single UAV, it is generally required that the vehicle holds a constant speed, thus $\dot{v}$ in (16) is equal to zero. However, if multiple UAVs are considered, the speed of

each vehicle should be adjusted to achieve the objectives of the coordination mission. At this moment, the computation of $\dot{v}$ is based on the coordination control law, which will be presented later in Section 3.3.

The following theorem provides the stability analysis of the MPF closed-loop system.

Theorem 1. *Consider the MPF problem subject to* (9) *and* (15). *The proposed MPF control law* (12) *and* (13) *ensure that* ${}^F x$, ${}^F y$ *and* $\tilde{\psi}$ *are bounded, while the equilibrium point* $e = 0$ *is globally uniformly asymptotically stable and locally exponentially stable.*

Proof. Consider the following Lyapunov function candidate.

$$V = \frac{1}{2}({}^F x^2 + {}^F y^2) + \frac{1}{2\gamma}\tilde{\psi}^2. \tag{17}$$

By differentiating (17) with respect to time and combining with (14), the following equation can be derived

$$\dot{V} = -k_1{}^F x^2 - \frac{k_2}{\gamma}\tilde{\psi}^2 + {}^F y v(\sin\bar{\psi}_d - \sin\zeta). \tag{18}$$

Using similar analyses with Wang and Wang (2017), it can be obtained that $\dot{V} \le 0$. From (17), it can be concluded that the signals ${}^F x$, ${}^F y$ and $\tilde{\psi}$ are all bounded. Applying the LaSalle's invariance principle leads to the conclusion that $e = 0$ is globally uniformly asymptotically stable.

Next, exponential stability of the closed-loop system will be proven. To facilitate analysis, (18) can be rewritten as

$$\dot{V} = -k_1{}^F x^2 - \frac{k_2}{\gamma}\tilde{\psi}^2 - f({}^F y){}^F y^2, \tag{19}$$

where $f({}^F y) = v\frac{\sin\zeta - \sin\bar{\psi}_d}{{}^F y}$. When ${}^F y > 0$, $\delta < 0$. Thus, $\zeta > \bar{\psi}_d$. As $|\zeta| < \frac{\pi}{2}$, $|\bar{\psi}_d| < \frac{\pi}{2}$ and $v > 0$, $f({}^F y) > 0$. Similarly, it can also be obtained that when ${}^F y < 0$, $f({}^F y) > 0$. Besides, when ${}^F y \to 0$, using L'Hospital's rule, it can be derived that $\lim_{{}^F y \to 0}f({}^F y) = \theta_\delta k_\delta\cos\zeta > 0$. It should also be noted that when ${}^F y \to \infty$, $f({}^F y) \to 0$. Based on the discussions above, it can be concluded that $\exists{}^F y_{oc} > 0$ and $k_3 > 0$, such that $f({}^F y) \ge k_3$, $\forall |{}^F y| \le {}^F y_{oc}$. Thus, $\dot{V} \le -k_1{}^F x^2 - \frac{k_2}{\gamma}\tilde{\psi}^2 - k_3{}^F y^2$, $\forall |{}^F y| \le {}^F y_{oc}$. According to Theorem 4.10 of Khalil (1996), it can be concluded that $e = 0$ is locally exponentially stable.

In practice, due to sensor limitations, wind information may not be accurately measured, resulting in bounded measurement error. In the sequel, robustness of our proposed control law will be briefly analyzed against wind measurement error. As the terms Σ, $\bar{\psi}_d$ and $\dot{\bar{\psi}}_d$ contain wind information, the proposed MPF control law (12) and (13) should be modified as $\dot{l} = v\cos\bar{\psi} + \hat{\Sigma} + k_1{}^F x$ and $\dot{\psi} = \omega_P + \kappa_l\dot{l} + \dot{\hat{\bar{\psi}}}_d - \gamma{}^F y v\frac{\sin\bar{\psi} - \sin\hat{\bar{\psi}}_d}{\bar{\psi} - \hat{\bar{\psi}}_d} - k_2(\bar{\psi} - \hat{\bar{\psi}}_d)$, where $\hat{\Sigma}$, $\dot{\hat{\bar{\psi}}}_d$ and $\hat{\bar{\psi}}_d$ are the estimations of their corresponding terms respectively. Consequently, the closed-loop system applying the above modified MPF control law can be given as follows.

$$\dot{e} = f(e) + g(e), \tag{20}$$

where $g(e) = [\tilde{\Sigma}, 0, -\dot{\tilde{\bar{\psi}}}_d - k_2\tilde{\bar{\psi}}_d + \gamma{}^F y v(\frac{\sin\bar{\psi} - \sin\bar{\psi}_d}{\bar{\psi} - \bar{\psi}_d} - \frac{\sin\bar{\psi} - \sin\hat{\bar{\psi}}_d}{\bar{\psi} - \hat{\bar{\psi}}_d})]^T$, $\tilde{\Sigma} = \Sigma - \hat{\Sigma}$, $\dot{\tilde{\bar{\psi}}}_d = \dot{\bar{\psi}}_d - \dot{\hat{\bar{\psi}}}_d$ and $\tilde{\bar{\psi}}_d = \bar{\psi}_d - \hat{\bar{\psi}}_d$. As $\tilde{\Sigma}$, $\dot{\tilde{\bar{\psi}}}_d$ and $\tilde{\bar{\psi}}_d$ are all bounded, $\exists e_r, g_\delta > 0$, such that $\|g(e)\| \le g_\delta$, $\forall e \in \{e \in \mathbb{R}^3 | \|e\| < e_r\}$. As $e = 0$ is a locally exponentially stable equilibrium point of system (14), using Lemma 9.2 in Khalil (1996) leads to the conclusion that bounded path following can be achieved with bounded wind measurement error. For the convenience of analysis, it is still assumed that wind information can be measured accurately in the following discussions.

3.2. Multi-UAV coordination

The previous subsection solves the MPF problem for a single UAV with arbitrary feasible speed profiles by proposing a non-singular MPF control strategy. When multiple UAVs are considered, the coordination problem should be addressed. To this end, the speeds of the vehicles are utilized at the coordination level, adapting based on the coordination information exchanged among vehicles.

Recall from Definition 2 that the main objective of the coordination task is to drive $\tilde{l}_i$ to zero for $i = 1, 2, \ldots, n$. To achieve this goal, l_i should be controlled. Thus, the coordination control variable for vehicle i can be defined as $u_i = \dot{l}_i$. To solve the coordination problem, the following control law is proposed.

$$u_i = \dot{l}_{i-1} - \beta \tanh(k_u \tilde{l}_i), \tag{21}$$

where β and k_u are positive constants. Based on (12), the speed of the ith vehicle is

$$v_i = \frac{u_i - \Sigma_i - k_1{}^F \dot{x}_i}{\cos \bar{\psi}_i}. \tag{22}$$

To satisfy the speed constraints, a necessary condition that should be guaranteed is that

$$\cos \bar{\psi}_i \geq c_1 > 0, \quad \forall t \geq 0, \quad i = 1, 2, \ldots, n, \tag{23}$$

where c_1 is a positive constant. In the next subsection, it will be discussed that the condition (23) can be guaranteed by using the proposed control method. Considering the Lyapunov function candidate $W_i = \frac{1}{2}\tilde{l}_i^2$, it can be obtained that

$$\dot{W}_i = -\beta \tilde{l}_i \tanh(k_u \tilde{l}_i) \leq 0. \tag{24}$$

According to the LaSalle's invariance principle, $\tilde{l}_i$ converges to zero asymptotically as $t \to \infty$.

3.3. Combined MPF and multi-UAV coordination

Sections 3.1 and 3.2 have addressed the MPF problem and the multi-UAV coordination problem separately, where the proposed MPF control law and the coordination control law can guarantee the asymptotic stability of the corresponding closed-loop systems respectively. However, for the MPF problem, the solution assumes that the speed of the vehicle satisfies the speed constraints, while the coordination control law is based on the assumption that the angle between the velocity vector of the vehicle and the tangent vector of the desired path is less than 90° (see (23)). To this end, this subsection addresses the stability and convergence issues of the combined MPF and multi-UAV coordination problem and derives conditions that guarantee the satisfaction of the speed constraints and collision-free maneuvers of the vehicles.

As mentioned in Remark 1, the computation of $\dot{v}$ in (16) is based on the coordination control law. Therefore, a complement of the MPF controller will be provided. In the sequel, $\dot{v}_i$ will be computed based on the coordination control law employed in this paper. From (22), $\dot{v}_i$ can be derived as

$$\dot{v}_i = \frac{\dot{u}_i - \dot{\Sigma}_i - k_1{}^F \dot{x}_i}{\cos \bar{\psi}_i} + v_i \dot{\bar{\psi}}_i \tan \bar{\psi}_i, \tag{25}$$

where $\dot{\Sigma}_i = -\dot{v}_d \cos(\psi_F - \psi_d) + v_d({}^F \omega_F - \dot{\psi}_d) \sin(\psi_F - \psi_d) - (\omega_P{}^F \omega_F \Delta y + \dot{\omega}_P \Delta x + \omega_P \Delta \dot{x}) \sin \psi_F + (\dot{\omega}_P \Delta y + \omega_P \Delta \dot{y} - \omega_P{}^F \omega_F \Delta x) \cos \psi_F$. It can be found that $\dot{\bar{\psi}}_i$ exists in the expression of $\dot{v}_i$. However, $\dot{v}_i$ is used to compute $\dot{\bar{\psi}}_{di}$ (see (16)), which is then utilized to derive $\dot{\bar{\psi}}_i$ (see (5) and (13)). For notational convenience, define $A_i = \dot{\delta}_i - \gamma^F y_i v_i \frac{\sin \bar{\psi}_i - \sin \bar{\psi}_{di}}{\bar{\psi}_i - \bar{\psi}_{di}} - k_2 \tilde{\psi}_i - \frac{\dot{\Delta}_i}{\sqrt{v_i^2 - \Delta_i^2}}$, $B_i = \frac{\Delta_i}{v_i \sqrt{v_i^2 - \Delta_i^2}}$, $C_i =$

$\frac{\dot{u}_i - \dot{\Sigma}_i - k_1{}^F \dot{x}_i}{\cos \bar{\psi}_i}$, $D_i = v_i \tan \bar{\psi}_i$. Based on (6), (13), (16), (25) and the definitions given above, the proposed MPF control law can be modified as

$$\dot{\bar{\psi}}_i = \omega_P + \kappa_l \dot{l} + \frac{A_i + B_i C_i}{1 - B_i D_i}. \tag{26}$$

To avoid singularity, the denominator $1 - B_i D_i$ is required to be bounded away from zero. As $1 - B_i D_i = 1 - \frac{\Delta_i}{\sqrt{v_i^2 - \Delta_i^2}} \tan \bar{\psi}_i \geq 1 - \frac{|\Delta_i|}{\sqrt{v_i^2 - \Delta_i^2}} |\tan \bar{\psi}_i| \geq 1 - \tan \theta_\zeta |\tan \bar{\psi}_i|$, a sufficient condition to guarantee that $1 - B_i D_i \geq c_2 > 0$, where c_2 is a positive constant, is

$$\tan \theta_\zeta |\tan \bar{\psi}_i| \leq 1 - c_2. \tag{27}$$

In this way, the singularity is avoided. In the sequel, it will be illustrated that (27) can be satisfied. Moreover, note that in (25), $\dot{u}_i$ is needed. From (21), it can be derived that $\dot{u}_i = \dot{u}_{i-1} - \beta k_u(u_i - u_{i-1})\text{sech}^2(k_u \tilde{l}_i)$, where $\dot{u}_{i-1}$ and u_{i-1} can be received from the $i - 1$th vehicle via wireless communication.

In the sequel, stability of the combined MPF and multi-UAV coordination system will be discussed. The following theorem summarizes the results.

Theorem 2. *Consider a fleet of n UAVs modeled by (1) coordinated using a pursuit strategy. Assume that all initial conditions satisfy the following inequalities.*

$$e_i(0) \in \Omega_c \triangleq \{e \in \mathbb{R}^3 | V \leq c^2\}, \tag{28}$$

$$|\tilde{l}_i(0)| \leq \bar{e}, \tag{29}$$

where c and $\bar{e}$ are positive constants, $c < \frac{\pi - 2\bar{\theta}}{2\sqrt{2\gamma}}$ and $\tan \theta_\delta \tan(\bar{\theta} + \sqrt{2\gamma}c) \leq 1 - c_2$ hold, V is the Lyapunov function defined in (17) and $i = 1, 2, \ldots, n$. Furthermore, the desired moving path satisfies (9), (15) and the following constraints.

$$\bar{v}_d + \bar{\omega}_P(\sqrt{\Delta x^2 + \Delta y^2})_{\max} \leq$$
$$\min\{c_1 v_{\max} - \sqrt{2}k_1 c - v_0 - \beta n - \bar{v}_w, \tag{30}$$
$$v_0 - v_{\min} - \sqrt{2}k_1 c - \beta n - \bar{v}_w\}$$

$$\min_{\Delta l - \bar{e} \leq \tau \leq \Delta l + \bar{e}} \|p_F(l) - p_F(l + \tau)\| \geq 2\sqrt{2}c + S, \tag{31}$$

where $\bar{v}_d$, $\bar{\omega}_P$ and $\bar{v}_w$ are the upper bounds of $|v_d|$, $|\omega_P|$ and $|v_w|$ respectively and $c_1 = \cos(\bar{\theta} + \sqrt{2\gamma}c)$. Then, the MPF control law (12) and (26) and the coordination control law (21) guarantee that ${}^F x_i$, ${}^F y_i$, $\tilde{\psi}_i$ and $\tilde{l}_i$ are bounded, e_i and $\tilde{l}_i$ converge to zero asymptotically, while the constraints $0 < v_{\min} \leq v \leq v_{\max}$ and $\|p_{i-1} - p_i\| \geq S$ are guaranteed.

Proof. First, we will show that for vehicle i, its speed v_i will not go outside the feasible range and its MPF errors will always remain inside the prespecified set Ω_c. From (22), (28) and (30), it can be obtained that when $t = 0$, the speed constraints for all vehicles are satisfied. Based on this preliminary result, the theorem will be proven by contradiction. To this effect, without loss of generality, consider that vehicle i violates the results of the theorem, which consists of the following three cases.

Case 1: For vehicle i, v_i does not satisfy $v_{\min} \leq v_i \leq v_{\max}$, while $e_i \in \Omega_c$ for all the time. As the speed constraints are satisfied at $t = 0$, it can be assumed that t' is the first time instant at which the speed constraints does not hold. Hence, $v_i(t') > v_{\max}$ or $v_i(t') < v_{\min}$ while $v_{\min} \leq v_i(t) \leq v_{\max}$ for $\forall t \in [0, t')$. In addition, $e_i \in \Omega_c$ for all the time. Thus, it can be obtained that $\|^F p_i\| \leq \sqrt{2}c$ and $|\tilde{\psi}_i| \leq \sqrt{2\gamma}c$ for $\forall t \geq 0$. As $\tilde{\psi}_i = \bar{\psi}_i - \bar{\psi}_{di}$ and $|\bar{\psi}_{di}| \leq \bar{\theta}$, we have $|\bar{\psi}_i| \leq \bar{\theta} + \sqrt{2\gamma}c$, resulting in $\cos \bar{\psi}_i \geq$

$\cos(\bar{\theta} + \sqrt{2\gamma}c) = c_1$, based on which (27) can be guaranteed as $\tan\theta_\delta \tan(\bar{\theta} + \sqrt{2\gamma}c) \le 1 - c_2$. Besides, consider Σ_i described in (6), which can be rewritten as $\Sigma_i = v_w \cos\bar{\psi}_{wi} - v_d \cos(\psi_d - \psi_{Fi}) - \omega_P\sqrt{\Delta x^2 + \Delta y^2}\cos(\psi_{Fi} + \varphi)$. Then, it can be easily obtained that $|\Sigma_i| \le \bar{v}_w + \bar{v}_d + \bar{\omega}_P(\sqrt{\Delta x^2 + \Delta y^2})_{\max}$. In addition, (21) can be rewritten in a matrix form as

$$\dot{\boldsymbol{l}} = \dot{l}_0 \mathbf{1}_n - \beta A^{-1}\tanh(k_u\tilde{\boldsymbol{l}}), \tag{32}$$

where $\boldsymbol{l} = [l_1, l_2, \ldots, l_n]^T$, $\tilde{\boldsymbol{l}} = [\tilde{l}_1, \tilde{l}_2, \ldots, \tilde{l}_n]^T$, $\tanh(\cdot)$ is an elementwise function and $\mathbf{1}_n$ is a $n \times 1$ vector with all one elements. Furthermore, $A = [a_{ij}]_{n\times n}$ is a $n \times n$ matrix with elements $a_{ij} = 1$ when $i = j$, $a_{ij} = -1$ when $i = j + 1$ and $a_{ij} = 0$ otherwise. From (32), it can be derived that $u_{i,\min} \le u_i \le u_{i,\max}$, where $u_{i,\min} = \dot{l}_0 - \beta i$ and $u_{i,\max} = \dot{l}_0 + \beta i$. Based on the discussions above, if the condition (30) is satisfied, it is straightforward to conclude that the speed constraints are satisfied at t', that is $v_{\min} \le v_i(t') \le v_{\max}$, which contradicts the claim that $v_i(t') > v_{\max}$ or $v_i(t') < v_{\min}$. Therefore, *Case 1* will not happen.

Case 2: For vehicle i, $\boldsymbol{e}_i$ does not remain inside Ω_c, while v_i satisfies $v_{\min} \le v_i \le v_{\max}$ for all the time. In this case, consider the Lyapunov function candidate V_i defined in (17) for vehicle i. As $\boldsymbol{e}_i(0) \in \Omega_c$ by assumption, and V_i is continuous and differentiable, there exists a time instant t' such that $V_i(t') = c^2$ and $\dot{V}_i(t') > 0$, while $V_i(t) \le c^2$, $\forall t \in [0, t')$. As in this case, the speed constraints are satisfied for all the time. Theorem 1 can be used to guarantee that, $\dot{V}_i(t) \le 0$, $\forall t \ge 0$, which leads to a contradiction. Therefore, this case will not happen as well.

Case 3: For vehicle i, both v_i violates $v_{\min} \le v_i \le v_{\max}$ and $\boldsymbol{e}_i$ does not remain inside Ω_c. Based on the fact that at the initial time instant both the speed constraints are satisfied and the MPF errors remain inside Ω_c, and the assumption that the speed constraints are violated for the first time at t' while the MPF errors first go outside Ω_c at t'', this case contains three subcases: (1) $t' < t''$; (2) $t' > t''$; (3) $t' = t''$. For subcase (1) and (2), a proof similar to that of *Case 1* and *Case 2* can be used to show that these two subcases will not happen. For subcase (3), it can be easily obtained that at time t', $v_i(t') > v_{\max}$ or $v_i(t') < v_{\min}$ while $v_{\min} \le v_i(t) \le v_{\max}$ for $\forall t \in [0, t')$ and $\boldsymbol{e}_i \in \Omega_c$ for $\forall t \in [0, t')$. Thus, it can be obtained that $\|{}^F\boldsymbol{p}_i\| \le \sqrt{2}c$ and $|\tilde{\psi}_i| \le \sqrt{2\gamma}c$ for $\forall t \in [0, t')$. Using a similar proof to the one of *Case 1*, it can be derived that the speed constraints are satisfied at time t', which is a contradiction. Therefore, this case will not happen as well.

Based on the discussions above, the speed constraints are satisfied and the MPF errors remain inside Ω_c for all the time. Thus the assumptions for both the MPF problem and the multi-UAV coordination problem can be satisfied. Therefore, it can be concluded that $\boldsymbol{e}_i$ and $\tilde{l}_i$ converge to zero asymptotically, while ${}^Fx_i$, ${}^Fy_i$, $\bar{\psi}_i$ and $\tilde{l}_i$ are bounded.

Next, collision avoidance among vehicles is analyzed. According to (24) and (29), it can be concluded that $|\tilde{l}_i(t)| \le \bar{e}$, $\forall t \ge 0$, thus, $\Delta l - \bar{e} \le l_{i-1} - l_i \le \Delta l + \bar{e}$. Hence, it can be obtained from (31) that $\|\boldsymbol{p}_{F,i-1} - \boldsymbol{p}_{Fi}\| \ge 2\sqrt{2}c + S$. As it has been derived that $\boldsymbol{e}_i$ for all i remain inside Ω_c, it is obvious that $\|\boldsymbol{p}_i - \boldsymbol{p}_{Fi}\| \le \sqrt{2}c$ and $\|\boldsymbol{p}_{i-1} - \boldsymbol{p}_{F,i-1}\| \le \sqrt{2}c$. Consequently, $\|\boldsymbol{p}_{i-1} - \boldsymbol{p}_i\| = \|\boldsymbol{p}_{i-1} - \boldsymbol{p}_{Fi} + \boldsymbol{p}_{Fi} - \boldsymbol{p}_i\| \ge \|\boldsymbol{p}_{i-1} - \boldsymbol{p}_{Fi}\| - \|\boldsymbol{p}_{Fi} - \boldsymbol{p}_i\| \ge \|\boldsymbol{p}_{i-1} - \boldsymbol{p}_{F,i-1} + \boldsymbol{p}_{F,i-1} - \boldsymbol{p}_{Fi}\| - \sqrt{2}c \ge \|\boldsymbol{p}_{F,i-1} - \boldsymbol{p}_{Fi}\| - \|\boldsymbol{p}_{i-1} - \boldsymbol{p}_{F,i-1}\| - \sqrt{2}c \ge S$. Therefore, collision avoidance between neighboring vehicles can be guaranteed.

4. Simulation results

This section presents the simulation results of a cooperative moving ground target tracking mission to demonstrate the efficacy of the proposed CMPF methodology. Consider two fixed-wing UAVs tracking a ground target which moves with speed v_d

and heading rate ω_d. It is assumed that $\{P\}$ is attached on the center of mass of the target with $\vec{x}_P$ pointing along the target velocity direction. The desired moving path is an ellipse described by ${}^Px_F = x_0 + a\cos\theta$ and ${}^Py_F = b\sin\theta$, where x_0, a, b are positive constants and θ is the parameter. Note that the desired path above is parameterized by θ. Through proper parameter transformations, ${}^P\boldsymbol{p}_F$ parameterized by l can also be obtained.

The parameters employed in the simulation are chosen according to the conditions listed in Theorem 2 and given as follows. The parameters of $\{P\}$ are set as $v_d = (4.9 + 0.1\sin(0.01t))$ m/s, $\omega_d = (0.005\cos(0.02t))$ rad/s, $x_0 = 223.6$ m, $a = 300$ m and $b = 200$ m. Wind parameters are chosen as $v_w = 1$ m/s and $\psi_w = -\frac{\pi}{4}$. The parameters for the proposed MPF control law are set as $\theta_\zeta = \frac{\pi}{8}$, $\bar{\theta} = \frac{\pi}{6}$, $k_1 = 0.1$, $\gamma = 0.00002$ and $k_2 = 6$. The parameters for the coordination control law are set as $v_0 = 30$ m/s, $\beta = 0.06$, $k_u = 1$ and $\Delta_l = 396.6$ m. The parameters for the speed constraints and the initial MPF errors are set as $v_{\min} = 20$ m/s, $v_{\max} = 50$ m/s, $c = 10$ and $\bar{e} = 10$. The sampling time of the simulation is set as 10 ms and the simulation period is 300 s. In the simulation, Euler method is utilized to solve the ordinary differential equations.

Fig. 2(a) explicitly shows the cooperative moving ground target tracking mission studied in the simulation. In this figure, the gray circle represents the target and the triangles denote two UAVs respectively. The black dashed, blue and green curves are the paths of the ground target and two UAVs respectively. This figure also plots the desired moving path at time instants 0s, 150s and 300s respectively, from which it can be found that two UAVs follow the desired moving path successfully. The MPF position and attitude errors of two UAVs are depicted in Figs. 2(b) and 2(c) respectively, which demonstrates the asymptotic convergence of the MPF errors. Fig. 2(d) depicts the inter-vehicle along-path distance between neighboring vehicles, from which it can be found that all the along-path distances between neighboring vehicles converge to the desired along-path separation distance asymptotically. The speeds and heading rates of the two UAVs are depicted in Fig. 2(e) and the Euclidean distance between two vehicles is shown in Fig. 2(f). From Fig. 2(e), it can be observed that the speed constraints are satisfied for both two vehicles and the heading rates of both vehicles are also in acceptable range. Fig. 2(f) demonstrates the collision-free maneuvers in the mission.

5. Conclusions and future work

This paper addresses the CMPF problem for multiple fixed-wing UAVs in the presence of stringent speed constraints and collision-free maneuver requirements. The methodology proposed in this paper extends the previous work on MPF for a single UAV to a more general setting that considers multi-UAV coordination as well as speed and spatial constraints. In the proposed framework, a non-singular MPF control law is derived such that the singularity problem existing in the previous work is avoided. Decentralized multi-UAV CMPF is achieved by adjusting the speed of each vehicle based on a pursuit strategy with the introduction of a virtual leader. This paper also provides conditions on initial MPF and coordination errors, wind speed as well as the motion information of the path transport frame, under which the combined MPF and multi-UAV coordination closed-loop system is stable and the MPF errors converge to zero asymptotically while speed constraints are satisfied and collision-free maneuvers can be guaranteed. Future work will investigate the robust MPF and CMPF control problem with unknown wind disturbance, which is considered to be a more challenging issue.
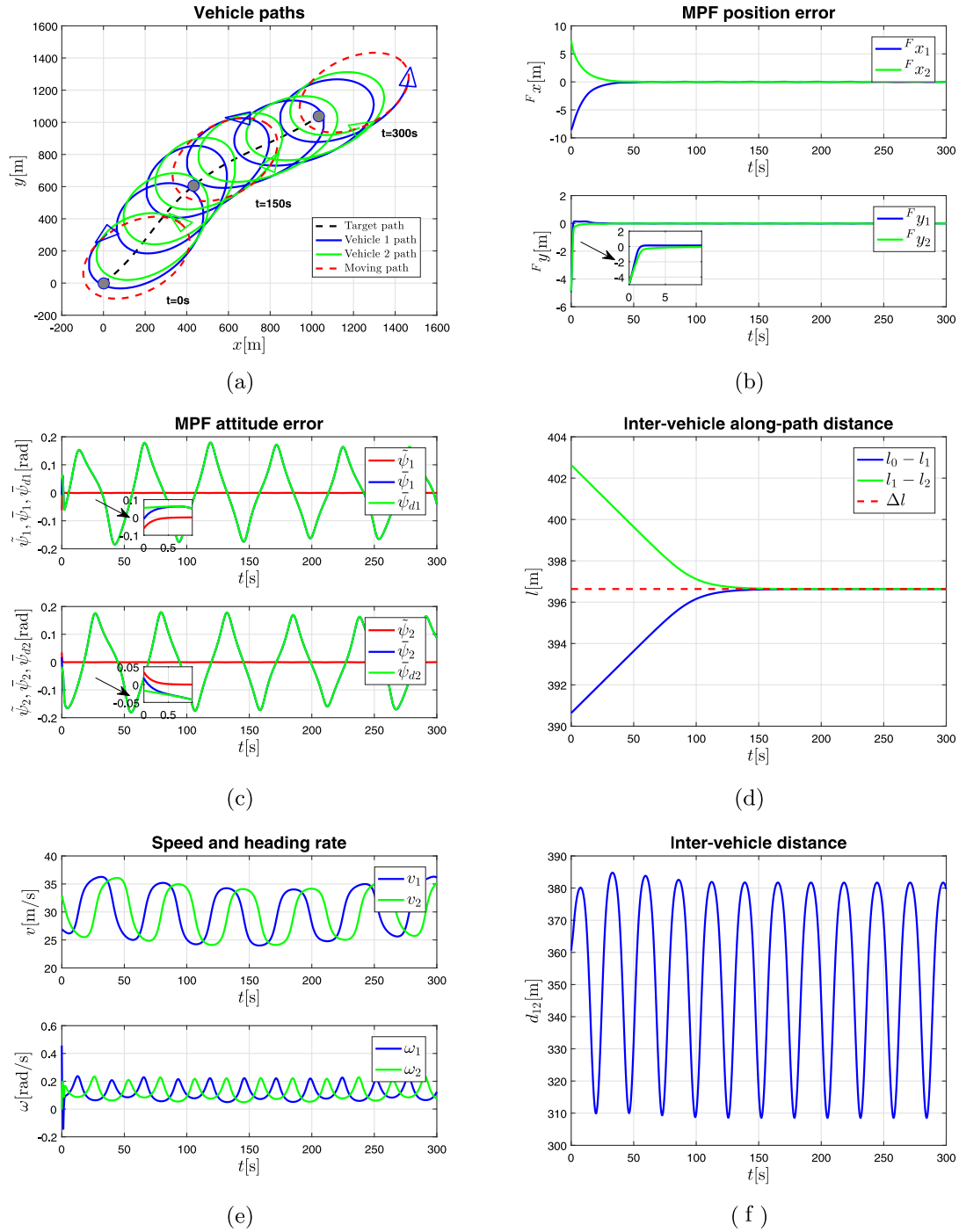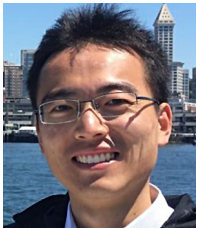
Fig. 2. Simulation results. (a) UAV paths in {I}. (b) MPF position error. (c) MPF attitude error. (d) Inter-vehicle along-path distance. (e) UAV speed and heading rate. (d) Inter-vehicle distance.

References

Beard, R. W., Ferrin, J., & Humpherys, J. (2014). Fixed wing uav path following in wind with input constraints. *IEEE Transactions on Control Systems Technology*, *22*(6), 2103–2117.

Cichella, V., Choe, R., Mehdi, S. B., Xargay, E., Hovakimyan, N., Dobrokhodov, V., et al. (2016). Safe coordinated maneuvering of teams of multirotor unmanned aerial vehicles: A cooperative control framework for multivehicle, time-critical missions. *IEEE Control Systems*, *36*(4), 59–82.

Cichella, V., Kaminer, I., Dobrokhodov, V., Xargay, E., Choe, R., Hovakimyan, N., et al. (2015). Cooperative path following of multiple multirotors over time-varying networks. *IEEE Transactions on Automation Science and Engineering*, *12*(3), 945–957.

Frew, E. W., Lawrence, D. A., & Morris, S. (2008). Coordinated standoff tracking of moving targets using lyapunov guidance vector fields. *Journal of Guidance, Control and Dynamics*, *31*(2), 290–306.

Griffiths, S. R. (2006). Vector field approach for curved path following for miniature aerial vehicles. In *Proceedings of the AIAA guidance, navigation, and control conference, volume 61* (pp. 63–64).

Khalil, Hassan K. (1996). *Noninear systems, vol. 2.* (pp. 1–5). New Jersey: Prentice-Hall, 5.

Lapierre, L., Soetanto, D., & Pascoal, A. (2003). Coordinated motion control of marine robots. In *Proc. 6th IFAC conference on manoeuvering and control of marine craft (MCMC)*.

Lapierre, L., Soetanto, D., & Pascoal, A. (2006). Nonsingular path following control of a unicycle in the presence of parametric modelling uncertainties. *International Journal of Robust and Nonlinear Control*, *16*(10), 485–504.

Micaelli, A., & Samson, C. (1993). Trajectory tracking for unicycle-type and two-steering-wheels mobile robots. Technical report.

Nelson, D. R., Barber, D. B., McLain, T. W., & Beard, R. W. (2007). Vector field path following for miniature air vehicles. *IEEE Transactions on Robotics*, *23*(3), 519–529.

Oliveira, T., Aguiar, A. P., & Encarnaçao, P. (2016). Moving path following for unmanned aerial vehicles with applications to single and multiple target tracking problems. *IEEE Transactions on Robotics*, *32*(5), 1062–1078.

Soetanto, D., Lapierre, L., & Pascoal, A. (2003). Adaptive, non-singular path-following control of dynamic wheeled robots. In *Decision and Control, 2003. Proceedings. 42nd IEEE Conference on, Volume 2* (pp. 1765–1770). IEEE.

Sujit, P. B., Saripalli, S., & Sousa, J. B. (2014). Unmanned aerial vehicle path following: A survey and analysis of algorithms for fixed-wing unmanned aerial vehicless. *IEEE Control Systems*, *34*(1), 42–59.

Summers, T. H., Akella, M. R., & Mears, M. J. (2009). Coordinated standoff tracking of moving targets: control laws and information architectures. *Journal of Guidance, Control and Dynamics*, *32*(1), 56–69.

Wang, Yuanzhe, & Wang, Danwei (2017). Non-singular moving path following control for an unmanned aerial vehicle under wind disturbances. In *Decision and control (CDC), 2017 IEEE 56th annual conference on* (pp. 6442–6447). IEEE.

Xargay, E., Dobrokhodov, V., Kaminer, I., Pascoal, A. M., Hovakimyan, N., & Cao, C. (2012). Time-critical cooperative control of multiple autonomous vehicles. *IEEE Control Systems Magazine*, *32*(5), 49.

Xargay, E., Kaminer, I., Pascoal, A., Hovakimyan, N., Dobrokhodov, V., Cichella, V., et al. (2013). Time-critical cooperative path following of multiple unmanned aerial vehicles over time-varying networks. *Journal of Guidance, Control and Dynamics*, *36*(2), 499–516.

Yu, Xiao, & Liu, Lu (2017). Cooperative control for moving-target circular formation of nonholonomic vehicles. *IEEE Transactions on Automatic Control*, *62*(7), 3448–3454.

Danwei Wang received his Ph.D. and M.S.E. degrees from the University of Michigan, Ann Arbor in 1989 and 1984, respectively. He received his B.E. degree from the South China University of Technology, China in 1982. He is a professor in the School of Electrical and Electronic Engineering, Nanyang Technological University (NTU), Singapore. He is the director of the STE-NTU Corp Lab, NTU. He has served as the head of the Division of Control and Instrumentation, NTU from 2005 to 2011 and the director of the Centre for System Intelligence and Efficiency, NTU until 2016. He also served as general chairman, technical chairman and various positions in several international conferences. He has served as an associate editor of Conference Editorial Board, IEEE Control Systems Society. He was an associate editor of International Journal of Humanoid Robotics and invited guest editor of various international journals. He was a recipient of Alexander von Humboldt fellowship, Germany. He has published widely in the areas of iterative learning control, repetitive control, fault diagnosis and failure prognosis, satellite formation dynamics and control, as well as manipulator/mobile robot dynamics, path planning, and control.

Yuanzhe Wang received his B.E. degree from the Southeast University, Nanjing, China, in 2010 and his M.Eng. degree from the Beihang University, Beijing, China, in 2013. He is currently a Research Associate and Ph.D. student in the School of Electrical and Electronic Engineering, Nanyang Technological University, Singapore. His current research interests include robot motion planning and control, multi-robot coordination and human–robot interaction.

Senqiang Zhu received his Ph.D. degree in robotics from Nanyang Technological University (NTU), Singapore, in 2014. He received his Bachelor and Master degrees both in mechanical engineering from Tsinghua University, China, in 2005 and 2007, respectively. From 2011 to 2015, he worked as a research associate and research fellow in NTU. In 2016, he was a robotics scientist and team leader in Singapore Eastern Robotics Company. Currently, he is a senior robotics scientist in International Intelligent Machines Pte. Ltd., Singapore. His research interests include robotics, UAV control theory and applications, as well as mobile robots.